ELSEVIER

Neurocomputing 38–40 (2001) 1335–1339

NEUROCOMPUTING

www.elsevier.com/locate/neucom

The prevalence of colinear contours in the real world

Matthias Kaschube[a,b,*], Fred Wolf[a], Theo Geisel[a], Siegrid Löwel[b]

[a]*Max-Planck-Institut für Strömungsforschung, D-37073 Göttingen, Germany*
[b]*Leibniz-Institut für Neurobiologie, D-39118 Magdeburg, Germany*

Abstract

Our visual system preferentially groups contour segments that not only have the same orientation but are colinear as well. Long-range horizontal connections are thought to play an important role in context-dependent modifications of neuronal responses. Since the topology of these connections shows a close relation to the perceptual grouping criterion of colinearity, we tested whether the statistical properties of real world images are biased towards colinear contours. By wavelet analysis we detected contours in images of natural environments and calculated their spatial correlations. In urban as well as in natural environments, the correlations between colinear contour segments were larger than the correlations for parallel contour segments. These observations indicate that colinear contour segments dominate real world images and thus might bias the functional and structural development of our visual system.

Keywords: Image analysis; Natural scenes; Wavelets; Visual cortex

1. Introduction

Both humans and other mammals (e.g. macaque monkeys and cats) are much better at detecting a contour composed of small oriented line segments that are oriented colinearly along the contour path than when the segments are aligned orthogonal to the contour. Therefore our visual system has the tendency to preferentially group contour segments that not only have the same orientation but are colinear as well. In the visual cortex, long-range horizontal connections span a cortical region much larger than the region which corresponds to the classical receptive field of an individual neuron. They are therefore thought to be involved in context-dependent

* Corresponding author. Max-Planck-Institut für Strömungsforschung, D-37073 Göttingen, Germany.

0925-2312/01/$ - see front matter
PII: S0925-2312(01)00493-3

modifications of neuronal responses. In addition, these connections preferentially link neurons with co-oriented, co-axially aligned receptive fields [4,1,6], suggesting a close relation between the topology of the connections and the perceptual grouping criterion of colinearity. To test whether colinearly oriented contours prevail in our visual environment, we quantitatively analyzed a set of real world images.

2. Methods

Natural scenes were chosen randomly from the collection of van Hateren [7]. Images were assigned to two different classes: (i) examples showing an outdoor urban area with streets and houses, and (ii) natural environments like forests, fields, grass and leaves. Images, which could not be assigned clearly to one of these two classes were not used. A total of 50 scenes for each setting was analyzed. Original images were rescaled at 512×512 pixels. Each pixel was a 2-byte unsigned integer with linear intensity. Images were calibrated to give zero mean and unit variance.

As a first step to find the orientation and intensity of contours, a reduced 2-dimensional real continuous wavelet analysis [2,3] was carried out for every image. Generally, wavelets with varying locations, orientations and scales are used to perform this kind of analysis. However, since our purpose was to detect rapid changes in luminance as the characteristic of contours, it was sufficient to use wavelets of a single scale, small enough for detecting rapid brightness differences. We tested wavelets with a typical wavelength of 4.5, 9 and 18 pixels. Generally they lead to similar results. In the following, we always used wavelets with a wavelength of 4.5 pixels. We calculated wavelet-coefficients for all translated and rotated wavelets given by

$$\tilde{I}(\mathbf{x},\theta) = \int_{\mathbb{R}^2} I(\mathbf{x}')\psi_{\mathbf{x}\theta}(\mathbf{x}')\,\mathrm{d}^2\mathbf{x}'.$$

Here, and in the following, the dependence on the scale is being suppressed. $\mathbf{x},\mathbf{x}' \in \mathbb{R}^2$, $\mathbf{x}$ is the position of the wavelet $\psi_{\mathbf{x}\theta}$ in image coordinates and $\theta \in [0,\pi]$ denotes its orientation. $\psi_{\mathbf{x}\theta}$ is defined through a mother wavelet $\psi(\mathbf{x}')$ by

$$\psi_{\mathbf{x}\theta}(\mathbf{x}') = \psi(\Omega^{-1}(\theta)[\mathbf{x}' - \mathbf{x}]),$$

with $\Omega(\theta)$ being the rotation matrix. For $\psi(\mathbf{x}')$ to be an admissible mother wavelet it is required that

$$\int_{\mathbb{R}^2} \psi(\mathbf{x}')\,\mathrm{d}^2\mathbf{x}' = 0.$$

To detect contour segments in the images it is necessary to use an anisotropic wavelet. Therefore, we used the anisotropic normalized Marr wavelet, first proposed by Jaffard [5]:

$$\psi(x,y) = \frac{1}{\sqrt{\frac{3}{4}\pi}} \exp\left(-\frac{1}{2}[x^2 + y^2]\right)(1 - x^2).$$

The orientations and intensities of contour segments within an image were represented by the wavelet coefficients $\tilde{I}(\mathbf{x},\theta)$.

In a second step, we calculated correlations between squared coefficients of the same θ. Since these correlations can be interpreted to represent correlations between equally oriented contour segments in the analyzed images, we will refer to the correlations as correlations between contour segments. We averaged correlations between equally oriented contour segments over all angles θ. In particular, correlations between contour segments which not only had equal orientation, but were also colinearly arranged, were compared with those between segments of the same orientation, but displaced in a direction orthogonal to their orientation. We will refer to the former as 'colinear' contour segments and to the latter as 'parallel' contour segments.

We calculated

$$C(\mathbf{r},\theta) = \langle E(\mathbf{x},\theta)\, E(\mathbf{x}+\mathbf{r},\theta)\rangle_{\mathbf{x}}.$$

Here $\langle\cdot\rangle_{\mathbf{x}}$ alternatively denotes averaging over positions $\mathbf{x}$ of an individual image or averaging over an ensemble of images. $E(\mathbf{x},\theta)$ are the squared and normalized wavelet coefficients. For fixed θ the correlation for colinear contour segments $C_{\mathrm{C}}(r,\theta)$ is a section of $C(\mathbf{r},\theta)$ in the direction $(r\cos\theta, r\sin\theta)$, while the correlation for parallel contour segments, $C_{\mathrm{P}}(r,\theta)$ is a section of $C(\mathbf{r},\theta)$ in the direction $(r\sin\theta, -r\cos\theta)$. Our analysis should not distinguish between different θ so we averaged over the angle to get the correlation for colinear and parallel contour segments:

$$C_{\mathrm{C}}(r) = \int\frac{\mathrm{d}\theta}{\pi} C(r\cos\theta, r\sin\theta,\theta),$$

$$C_{\mathrm{P}}(r) = \int\frac{\mathrm{d}\theta}{\pi} C(r\sin\theta, -r\cos\theta,\theta).$$

3. Results

We used a reduced wavelet analysis to detect contour segments in natural images and calculated correlations between iso-oriented contour segments. The correlations between colinear contour segments were compared to the correlations between parallel contour segments.

Fig. 1 shows two examples. On the left side, some houses are displayed. On the right side, a part of undergrowth is depicted. Beneath, corresponding correlation functions of colinear and parallel contour segments are shown on logarithmic scales.

For both images, correlations for colinear contours $C_{\mathrm{C}}(r)$ were typically larger than correlations for parallel contour segments $C_{\mathrm{P}}(r)$. $C_{\mathrm{P}}(r)$ appeared to be less regular than $C_{\mathrm{C}}(r)$.

Fig. 2 depicts the average correlation functions taken over all analyzed images within the two classes. The upper diagram corresponds to urban environments. The lower diagram corresponds to natural environments. For both settings, correlations of colinear contour segments are typically larger than correlations for parallel contour

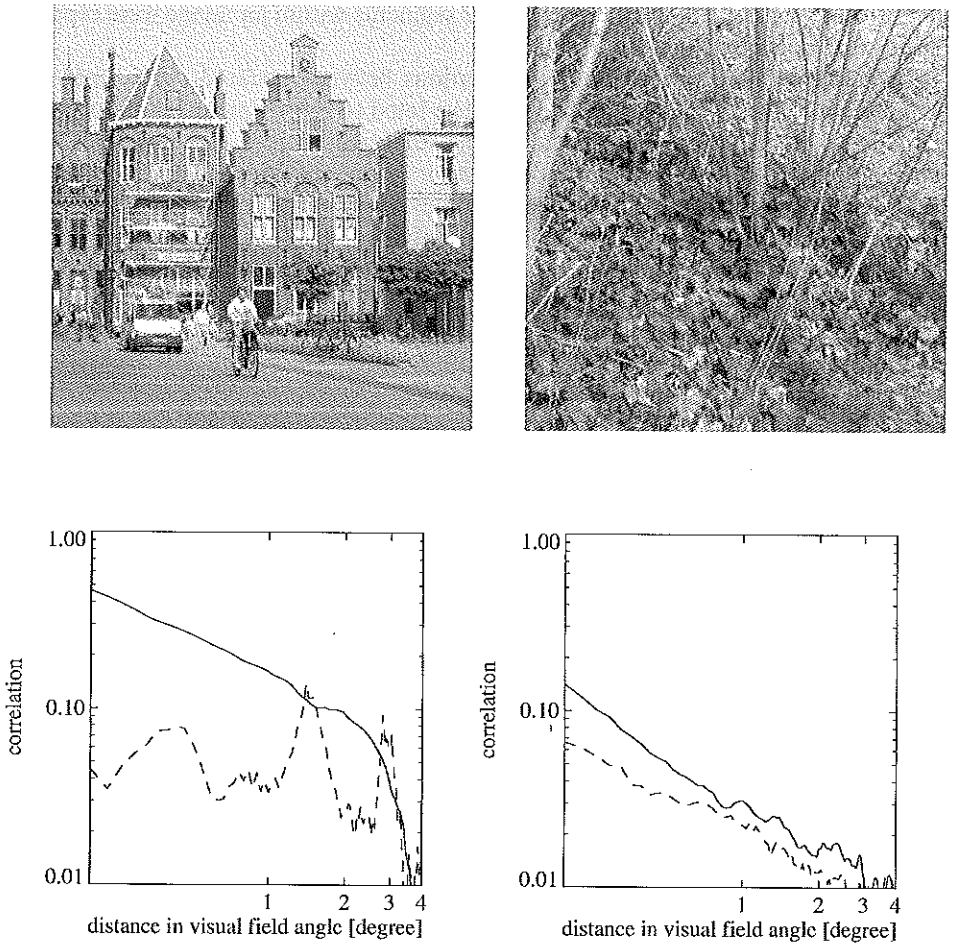

Fig. 1. Two typical visual scenes and their correlation functions. Some houses are displayed on the left side; a part of undergrowth is displayed on the right side. Below the two images correlation functions are shown on logarithmic scales. The correlations for colinear contour segments $C_C(r)$ are represented by the solid lines. The correlations for parallel contour segments $C_P(r)$ are represented by the dashed lines. Note that $C_C(r)$ is typically larger than $C_P(r)$ and decays more regular than $C_P(r)$.

segments. The effect is more pronounced in urban environments than in natural environments.

4. Conclusions

In urban as well as in natural environments, the correlations between colinear contour segments were larger than the correlations for parallel contour segments.

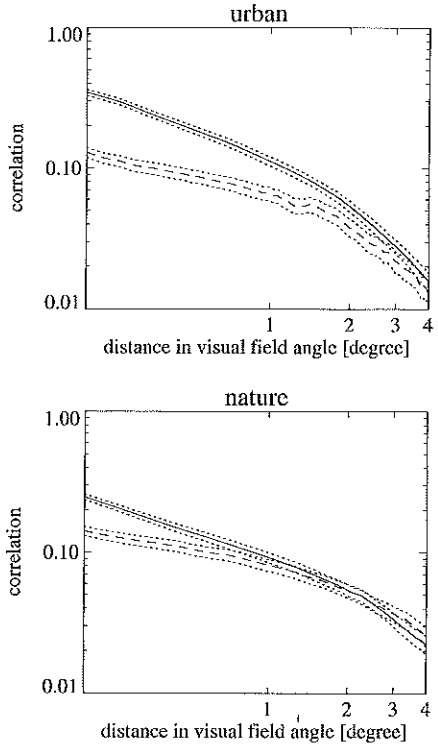

Fig. 2. Correlation functions $C_C(r)$ and $C_P(r)$ averaged over 50 scenes for each setting. The upper diagram displays correlation functions for urban environments. The lower diagram displays correlation functions for natural environments. Correlation functions are shown on logarithmic scales. Solid lines represent the correlation functions for colinear contour segments $C_C(r)$. Dashed lines represent the correlation functions for parallel contour segments $C_P(r)$. Error bars are indicated by the dotted lines. Note that for both settings $C_C(r)$ is larger than $C_P(r)$ over two orders of magnitude in distance.

These observations indicate that colinear contour segments dominate real world images and thus might bias the functional and structural development of our visual system.

References

[1] W.H. Bosking, Y. Zhang, B. Schofield, D. Fitzpatrick, J. Neurosci. 1 (1997) 263–268.
[2] I. Daubechies, Ten Lectures on Wavelets, CBMS Lecture Notes Series, SIAM, 1991.
[3] M. Farge, Ann. Rev. Fluid Mech. 24 (1992) 395–457.
[4] D. Fitzpatrick, Cerebral Cortex 6 (1996) 329–341.
[5] S. Jaffard, Wavelets, Fractals, and Fourier Transforms, 1991, pp. 47–64.
[6] K.E. Schmidt, R. Goebel, S. Löwel, W. Singer, Europ. J. Neurosci. 9 (1997) 1083–1089.
[7] J.H. van Hateren, A. van der Schaaf, Proc. R. Soc. London 265 (1998) 359–366.